IEEE Access
Multidisciplinary | Rapid Review | Open Access Journal

Received 10 September 2023, accepted 10 October 2023, date of publication 16 October 2023, date of current version 23 October 2023.

Digital Object Identifier 10.1109/ACCESS.2023.3324820

RESEARCH ARTICLE

Invariant Set-Based DC Microgrid Decentralized Actuator Fault-Tolerant Control

HISHAM M. SOLIMAN[1], EHAB H. E. BAYOUMI[2], FARAG ALI EL-SHEIKHI[3], RAZZAQUL AHSHAN[4], (Senior Member, IEEE), SARVAR HUSSAIN NENGROO[5,6], AND SANGKEUM LEE[7]

[1]Department of Electrical Power Engineering, Faculty of Engineering, Cairo University, Giza 12613, Egypt
[2]Department of Mechanical Engineering, Faculty of Engineering, The British University in Egypt (BUE), El Sherouk, Cairo 11837, Egypt
[3]Department of Electrical and Electronics Engineering, Istanbul Esenyurt University, 34517 Esenyurt, Istanbul, Turkey
[4]Department of Electrical and Computer Engineering, College of Engineering, Sultan Qaboos University (SQU), Muscat 123, Oman
[5]Cho Chun Shik Graduate School of Mobility, Korea Advanced Institute of Science and Technology (KAIST), Yuseong-gu, Daejeon 34141, South Korea
[6]Department of Engineering Technology, Technical University of Denmark (DTU), Ballerup, Denmark
[7]Department of Computer Engineering, Hanbat National University, Daejeon 34158, South Korea

Corresponding authors: Razzaqul Ahshan (razzaqul@squ.edu.om) and Sangkeum Lee (sangkeum@hanbat.ac.kr)

ABSTRACT Faults and system failure components are primarily two causes of unstable or deteriorating control performance of power system. In this study, we present a novel approach to the decentralized restoration of large DC microgrids using fault-tolerant control (FTC). The microgrid achieves decentralization by partitioning into several smaller grids. Each independent grid views the actions of the other grids as an external disturbance. The malfunction of the controller is represented in the input matrix as a norm-bounded uncertainty. The disturbance impact is diminished due to the proposed invariant-set approach. The proposed control can address simultaneous failures in actuators with random placement and degradation levels. In a passive FTC system, when the defect cannot be detected (or the fault may not have been clearly addressed), the proposed technique is utilized. After the fault has occurred, it can be viewed as an uncertainty in system dynamics. The controller that stabilizes the system is obtained by solving iteratively bilinear matrix inequalities as linear matrix inequalities. In addition, this study presents and discusses positive outcomes of applying this method to a system of six interconnected DC microgrids in the event of multiple fault types. The proposed control successfully stabilizes the severe case of simultaneous actuator faults.

INDEX TERMS DC microgrid (MG), decentralized control, fault-tolerant control, invariant ellipsoid, robust tracker.

I. INTRODUCTION

A. BRIEF SURVEY

The different components in the classical control theory are assumed to be reliably operated. This is not a practical assumption as any component in the system may fail or be mal-operated at any time. Maintaining system stability and performance as well as fault determination are the main roles of the control system. To provide maintenance as well as to avoid faults, a monitoring and diagnostic approach is required. Power systems stabilization under random line failure or unreliable operation is given [1], [2]. These can be defined as fault-tolerant control systems (FTCs) [3], [4]. The basic assembly of FTCS is shown in Figure 1.

The two main types of fault-tolerant control system can be classified as active and passive control system [3], [4], [5], [6], [7]. In the active fault-tolerant control (AFTC), different kinds of faults can be managed which leads to perfect system execution. The fault detection and isolation (FDI) module, which is a reconfiguration system and an adjustable controller in itself, is responsive to the outcome that is sought. AFTC and FDI are crucial in identifying and isolating defective elements to increase adaptation in defective conditions [7]. Passive fault tolerant control (PFTC) is faster than AFTCS because it lacks an FDI unit and is computationally simpler than AFTCS.

The associate editor coordinating the review of this manuscript and approving it for publication was Mou Chen.

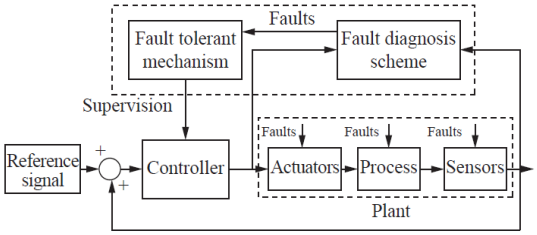

FIGURE 1. Basic architecture of FTCS.

Although passive FTC systems are less sophisticated, they are cautious to account for ''worst case'' fault consequences [8]. Passive FTC has been designed using variety of methods. Among those techniques are sliding mode control (SMC) method [8], H∞ [9], linear quadratic control [3], fuzzy logic control [10], Lyapunov-based control [11], and control allocation [12]. Such passive FTC systems are typically less complex and are common due to their design simplicity and use [13].

Following is a summary of the many fault compensation strategies utilized in active FTC design:

Active FTC system's techniques are based on real-time fault isolation and detection. Switching-Based active FTC, according to the fault kind and severity, the system switches between a collection of preconfigured candidate controllers that make up the active FTC controller. Reference [14] describes an active FTC method that addresses the dwell time among switches. By resolving linear matrix inequality, the system stability is ensured.

The design methods of AFTC require the least amount of delay and the highest level of FDI data. To find errors, an adaptive neural network (NN) technique is used [15]. A nonlinear observer was introduced and integrated with a NN based on the observer's nonlinear model, while its gains were updated using an extended Kalman filter (EKF). A wavelet-based active FTC system for a multi-agent leader-following system was developed in [16].

AFTC systems' disadvantages can be classified as follows:

(1) delayed detection and isolation. As faults are detected after their occurrence, the controller is reconstructed to compensate for the fault. The controller can then be precisely designed to the system with the fault dynamics.

(2) the resulting AFTC controller is more complex than PFTC.

(3) fault detection is a difficult problem and cannot assure a precise detection in presence of external disturbances.

Through extensive implementation of the Microgrids (MGs) power in distribution networks, a reduction in pollution, minimizing the transmission system losses, improving the system reliability, and enhancing stability can be obtained [17]. The MG can be operated in an isolated mode or connected to the utility grid. MGs can be classified as direct current DC, alternating current AC, or hybrid DC/AC. Because of the fundamental advantages of the Direct Current (DC) system in terms of compatibility with power generation sources, modern loads, and storage devices, DC MG has become popular over Alternate Current (AC) system. Due to the above reasons, the research work in this article concentrates on faults that may occur in DC MG. The control of the voltage, frequency, active and reactive power are the main challenges related to the MGs. Operating modes of MG can be islanded or grid-connected. The MG faults could be faults in the actuators, sensors, communication system, and in the plant itself.

To achieve various control objectives in DC MGs, there are many approaches for using three-level hierarchical structure which are primary control, secondary control, and tertiary control. The primary, secondary and tertiary control are responsible for the regulation of voltage, restoration of voltage, and power management respectively [18], [19].

The MGs can also be categorized in terms of communication, where, the primary factor in control is communication. Three methods—distinguished by the degree of communication—are used to achieve the fundamental control [20], and they are as follows:

Centralized, decentralized and distribution control

Distributed generators are regulated by a central controller in this control scheme. Digital Communication Links (DCLs) are used to collect, process, and send data from the DC MG's units back to the controller. The central control system's beating heart is communication. The robust observability and controllability of the entire system are one of this scheme's benefits. The system's single point of failure, as well as its decreased reliability, adaptability, and scalability, are only a few of its many drawbacks. A common illustration of a centralized control technique is the main/secondary control system.

There is no communication link in this system. The distributed generators are managed by independent controllers through their local variables. The fact that it does not require any communication linkages between the various system elements makes it the most reliable control approach. Decentralized control, however, has some performance limitations.

The advantages of both centralized and decentralized control techniques are combined in this control system. Each unit's controller only uses the few available DCLs to exchange data with its immediate neighbors. In light of these goals, state of charge, voltage restoration, current sharing, and proportional load power sharing can easily be performed.

B. PAPER CONTRIBUTION

The method introduced in this paper addresses the decentralization restriction by offering a sophisticated method of adding actuator malfunction into the passive FTC framework. A robust fault-tolerant control for linear discrete-time systems is the focus of this manuscript. Moreover, it applies an ellipsoidal bound to a robust invariant set. The most important thing is to keep the system's state within the robust invariant feasible set which is a collection of states that ensures the

stability of the suggested control technique. Minimizing the invariant ellipsoid volume improves the system's performance by attenuating the disturbance consequence.

The main contributions of this study are:

1. The invariant ellipsoid approach is used for introducing robustness against external disturbances and fault uncertainty.
2. The development of robust invariant set is based on quadratic boundedness.
3. Unlike the active FTC approach which requires fault detection and two-components control, the proposed control is a simple proportional feedback state and easy to implement.
4. The proposed control can also handle simultaneous actuator faults (extremely uncommon in practice).

C. PAPER ORGANIZATION

The following is how the paper is set up: A general outline of the suggested structure is presented in Section II. In Section III, passive fault tolerant control is introduced. It describes the fault-tolerant mechanism and the robust control technique. The resilient invariant-ellipsoid set notion and its derivation are presented in Section IV. Section V presents the suggested effective robust control for linear systems. The six-connected DC microgrid system is an example given in the final part as an illustration.

Notation: The term "matrix transposition" is denoted by the superscript $(\cdot)'$ throughout the text, while R^n stands for the n-dimensional Euclidean space and $R^{n\times m}$ refers to the collection of all $n\times m$ real matrices. Vectors are designated by small letters, scalers by small Greek letters, and matrices by capital letters. A symmetric $P \in R^{n\times m}$, $P > (<)0$ indicates that it is a positive (negative) definite. A symmetric matrix $\begin{bmatrix} Q & R \\ R' & P \end{bmatrix}$ is denoted by $\begin{bmatrix} Q & R \\ * & P \end{bmatrix}$. Likewise, $(M+N+*)$ means that $(M+N+M'+N')$. Lastly, 0 and I represent the zero matrices and the identity matrix, respectively.

Fact 1 [4]: For any real matrices Γ, Δ, E with suitable dimensions and $\Delta'\Delta \leq I$, this means that:

$$\Gamma\Delta E + * \leq \varepsilon\Gamma\Gamma' + \varepsilon^{-1}E'E, \forall\varepsilon > 0$$

Fact 2 [4] (Schur Complement): This fact is used to transform a nonlinear matrix inequality to a linear one.

Given constant matrices W_1, W_2, W_3 where $W_1 = W'_1$, and $0 < W_2 = W'_2$. Then

$$W_1 + W_3'W_2^{-1}W_3 < 0 \Leftrightarrow \begin{bmatrix} W_1 & \bullet \\ W_3 & -W_2 \end{bmatrix} < 0$$

II. PROBLEM FORMULATION

Consider a large system that has been linearized with a Taylor expansion around an operating point. A discrete linear state space representation of the linearized system with a sampling period T_s is given by

$$x(k+1) = Ax(k) + Bu(k), \quad y(k) = Cx(k) \tag{1}$$

where $A \in R^{n.n}$, $B \in R^{n.m}$, $C \in R^{l.n}$. Assuming all the states are available for state-feedback control, $C{=}I$.

The number of outputs that can track a reference input vector, y_r, cannot be more than the number of control inputs to maintain controllability [6]. Consequently, the output equation for the open-loop system shown by (1) can be rewritten as

$$y(k) = Cx(k) = \begin{bmatrix} C_1 \\ C_2 \end{bmatrix} x(k) = \begin{bmatrix} y_1(k) \\ y_2(k) \end{bmatrix} \tag{2}$$

where $y_1 \in R^h, h \leq l$ denotes the vector of the outputs required to follow the reference input vector y_r.

A. DECENTRALIZED ROBUST FTC TRACKING AND ACTUATOR FAULT REPRESENTATION

A decentralized approach is preferable to be used for controlling large systems. This is because it avoids using a communication network to send the states to the computer (as in centralized control), delays, packet loss, and failure in the hub computer…etc. The global system (1) with $C = I$

$$x(k+1) = Ax(k) + Bu(k) \tag{3}$$

can be decomposed into N subsystems. With $A = \{A_{i,j}\}$, and $B = blockdiagonl\{B_1..B_N\}$ the subsystem #i is given by

$$\begin{aligned} x_i(k+1) &= A_{ii}x_i(k) + B_iu_i(k) + D_ix(k), D_i \\ &= \begin{bmatrix} A_{i1} \ldots & O_{ii} \ldots A_{iN} \end{bmatrix}, \quad i = 1..N \end{aligned} \tag{4}$$

The dimensions of x_i, u_i are respectively $n_i, m_i, n = \sum_{i=1}^{N} n_i, m = \sum_{i=1}^{N} m_i$,

Assuming $x(k)$ as a bounded external disturbance $w(k)$,

$$\|w(k)\| \leq 1 \tag{5}$$

Note that if the disturbance norm is >1, the disturbance matrix D_i can always be scaled such that the constraint (5) is satisfied. (e.g. if $D_{old}\ w(k)$, $\|w(k)\| = 2$, we can select $D_{new} = 2D_{old}$). When fault occurs in actuator #i, equation (4) which represents subsystem# i becomes

$$\begin{aligned} x_i(k+1) &= A_{ii}x_i(k) + (B_i + \Delta B_i)u_i(k) + D_iw(k), \\ & k = 0, 1, 2\ldots, \ i = 1..N \end{aligned} \tag{6}$$

where

$$\Delta B_i = B_i.diag(\beta(k)) = B_i.\Delta_B(k)$$

When a fault occurs in actuator # i, at channel j,$j{=}1..m_i$, then $\beta = \begin{bmatrix} \beta_1..\beta_j \ldots \beta_{m_i} \end{bmatrix}$, $\beta_j \in]0..-1]$. Let diag(β(k)) be denoted as $\Delta_B(k)$. When β_j = -1,means complete failure of channel j in actuator # i. For partial actuator fault, $0 < \beta_j < 1$. For example, when an abrupt decrease of 70% in the effectiveness of actuator i, $\beta_i = 0.3$. Note that the uncertainty is norm-bounded given by $\|\Delta_B(k)\| < 1$. There are two models to describe the faults, additive and multiplicative. The last equation describes the actuator fault as an additive uncertainty which tackles easily such type of fault.

To achieve tracking task for subsystem i, a vector comparator and integrator are added z_i which fulfills:

$$z_i(k+1) = z_i(k) + T_s[y_{ri}(k) - y_{1i}(k)] \tag{7}$$

where T_s is the sampling period. As a result, the augmented state space representation controls the open-loop system of subsystem i

$$\hat{x}_i(k+1) = \hat{A}_{ii}\hat{x}(k) + \hat{B}_i u_i(k) + \hat{D}_i w(k) + \hat{I}_i y_{ri}(k), \tag{8}$$

where

$$\hat{x}_i = \begin{bmatrix} x_i \\ z_i \end{bmatrix}, \quad \hat{A}_{ii} = \begin{bmatrix} A_{ii} & O \\ -T_s C_{1i} & I_i \end{bmatrix}, \quad \hat{B}_i = \begin{bmatrix} B_i \\ O \end{bmatrix},$$
$$\hat{D}_i = \begin{bmatrix} D_i \\ O \end{bmatrix}, \quad \hat{I}_i = \begin{bmatrix} O \\ T_s I_i \end{bmatrix},$$

It is required to design the state feedback control given by

$$u_i(k) = \hat{K}_i(k)\hat{x}_i(k) = \begin{bmatrix} K_{1i} & K_{2i} \end{bmatrix}\hat{x}_i(k) \tag{9}$$

Matrix C is an identity matrix for this application. The state variables are the outputs.

III. PASSIVE FAULT TOLERANT CONTROL

To design PFTC, the invariant ellipsoid set is first introduced in this section.

A. INVARIANT ELLIPSOID SET [21]

The ellipsoid set

$$E = x'(k) P^{-1} x(k) \le 1, \quad P > 0 \tag{10}$$

centered at the origin is said to be state-invariant for the discrete-time dynamic system

$$x(k+1) = Ax(k) + Bu(k) + Dw(k), \text{ subject to} \|w(k)\| \le 1 \tag{11}$$

if the condition $x_0 \in E$ implies $x(k) \in E$ for all future instants $k = 1, 2, \ldots$. In other words, if the state trajectory $x(k)$ lies inside E, it will not leave the ellipsoid in the future time. The pair (A, B) is assumed controllable.

An invariant ellipsoid is also attracting in the sense that any trajectory started from a point outside E will be attracted by this ellipsoid as time evolves.

Theorem 1 ([21]): Let P, Y be a solution to the minimization problem

$$\begin{aligned} &\textit{minimize } tr\ P \\ &\text{subject to } \begin{bmatrix} -\alpha P & * & * \\ AP + BY & -P & * \\ 0 & D' & -(1-\alpha) I \end{bmatrix} \le 0 \end{aligned} \tag{12}$$

for some $0 < \alpha < 1$. The resultant state feedback controller is given by

$K = YP^{-1}$.

Proof: see Appendix.

Based on theorem 1, the next theorem is derived to solve the passive FTC problem.

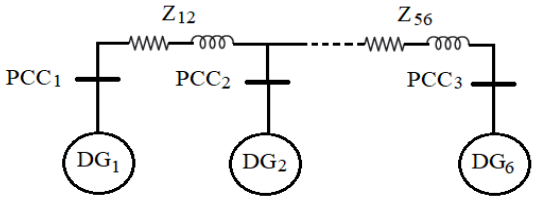

FIGURE 2. Six DGs islanded DC-microgrid.

Theorem 2: For subsystem i, let P_i, Y_i, scalar α be a solution for

$$\begin{aligned} &\textit{minimize } tr(P_i) \\ &\text{Subject to} \\ &\begin{bmatrix} -\alpha P_i & * & * & * \\ \hat{A}_{ii}P_i + \hat{B}_i Y_i & -P_i + \epsilon \hat{B}_i \hat{B}_i' & * & * \\ 0 & \hat{D}_i' & -(1-\alpha) I_i & * \\ Y_i & 0 & 0 & -\epsilon I \end{bmatrix} \le 0, \\ &\epsilon > 0, 0 < \alpha < 1 \end{aligned} \tag{13}$$

Then the FTC is

$$\hat{K}_i = Y_i P_i^{-1}$$

The above matrix inequality is nonlinear due to the term αP_i. It is a bilinear matrix inequality BMI which is difficult to be solved. However, it can be transformed into a linear matrix inequality LMI which is easy to solve by fixing the scalar α. The above optimization problem is done by updating α iteratively on an outer loop to minimize $tr(P_i)$.

Proof:

$$\begin{bmatrix} -\alpha P_i & * & * \\ \hat{A}_{ii}P_i + (\hat{B}_i + \Delta\hat{B}_i)Y_i & -P_i & * \\ 0 & \hat{D}_i' & -(1-\alpha) I_i \end{bmatrix} \le 0$$

$$\therefore \begin{bmatrix} -\alpha P_i & * & * \\ A_{ii}P_i + B_i Y_i & -P_i & * \\ 0 & \hat{D}_i' & -(1-\alpha) I \end{bmatrix}$$

$$+ \left(\begin{bmatrix} 0 \\ B_i \\ 0 \end{bmatrix} \Delta_B \begin{bmatrix} I & 0 & 0 \end{bmatrix} Y_i + * \right) \le 0 \text{ or},$$

$$\times \begin{bmatrix} -\alpha P_i & * & * \\ A_{ii}P_i + B_i Y_i & -P_i & * \\ 0 & \hat{D}_i' & -(1-\alpha) I \end{bmatrix}$$

$$+ \epsilon \begin{bmatrix} 0 & 0 & 0 \\ 0 & B_i B_i' & 0 \\ 0 & 0 & 0 \end{bmatrix} + \frac{1}{\epsilon} \begin{bmatrix} Y_i' \\ 0 \\ o \end{bmatrix} \begin{bmatrix} Y_i & 0 & 0 \end{bmatrix} + * \le 0$$

Using Fact 1, we get

$$\begin{bmatrix} -\alpha P_i & * & 0 & * \\ A_{ii}P_i + B_i Y_i & -P_i + \epsilon B_i B_i' & D & * \\ 0 & \hat{D}_i' & -(1-\alpha) I & * \\ Y_i & 0 & 0 & -\epsilon I \end{bmatrix} \le 0, \epsilon > 0$$

This completes the proof.

If the operating point of the DC MG changes due to load variations, the linearized model around the operating point

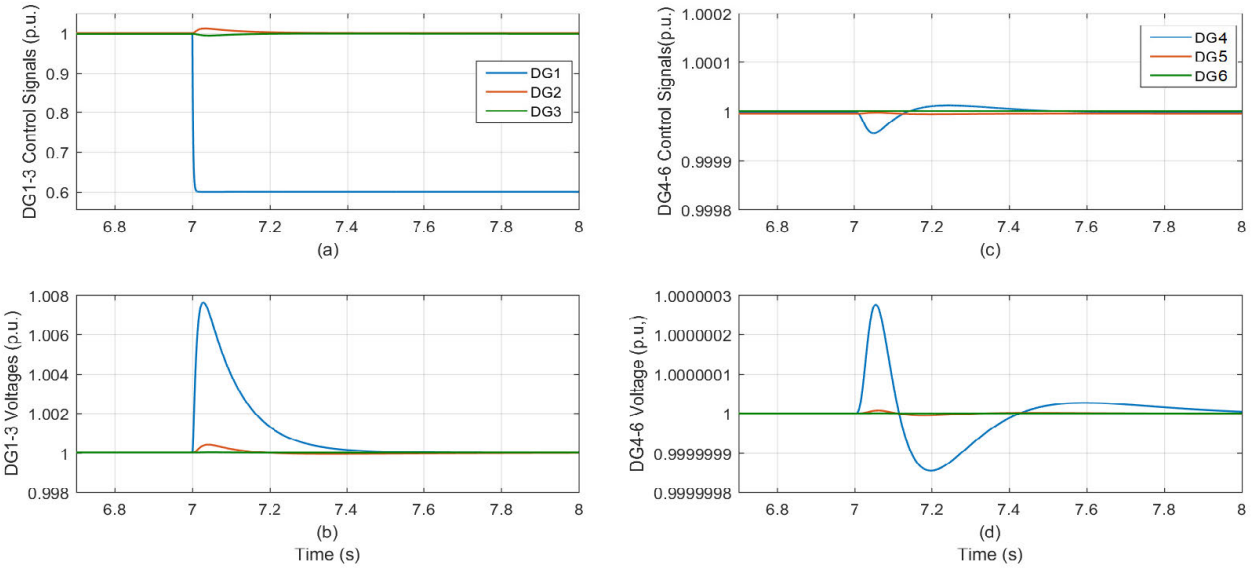

FIGURE 3. Degradation in the control signal of DG1 from 100% to 60%. (a) control signals for DG1, DG2 and DG3. (b) controlled output voltages of DG1, DG2 and DG3. (c) control signals for DG4, DG5 and 6. (d) controlled output voltages of DG4, DG5 and DG6.

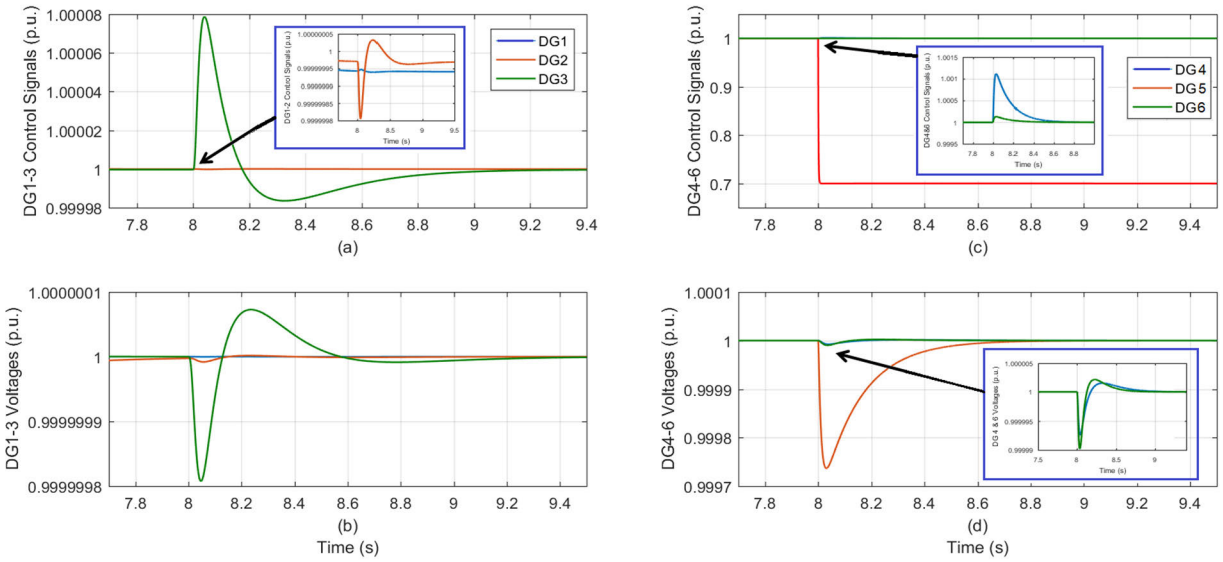

FIGURE 4. Degradation in the control signal of DG5 from 100% to 70%. (a) control signals for DG1, DG2 and DG3. (b) controlled output voltages of DG1, DG2 and DG3. (c) control signals for DG4, DG5.

also changes. This results in system uncertainties of the form $\Delta\hat{A}_{ii} = F_A\Delta_A H_A$, *and* $\Delta\hat{D}_i = F_D\Delta_D H_D$. The uncertainties are represented in the norm-bounded form

$$\|\Delta_A\| \leq 1, \|\Delta_D\| \leq 1$$

In this case, the fault-tolerant controller is given by the following theorem.

Theorem 3: For subsystem i, let P_i, Y_i, scalar α be a solution, as shown in the equation at the bottom of the next page.

Then the FTC is $\hat{K}_i = Y_i P_i^{-1}$

Proof: Shown in the equation at the bottom of the next page.

Fact 2 (Schur complement) is used in the above proof.

IV. MICROGRID STUDY SYSTEM

Fig. 2 presents the study system that consists of six DG in an islanded DC microgrid. The contiguous-time state model of the study system [22], is discretized with a sampling time of 0.001s. The DC MG's discrete-time model is as follows, as shown in the equation at the bottom of page 7.

Decomposing the state equation above for the Six DGs islanded DC-MG into 6 sub-grids, and solving Theorem 2 for each, we get the decentralized passive FTC as follows in Table 1.

The Matlab/SimPower Systems Toolbox is used to model the study system. According to the IEEE standards in [23], robust stability, mandatory response, and steady-state

TABLE 1. Proposed decentralized passive FTC.

Sub-grid #	α	Min. Ellipsoid vol.	Controller[K_x ,K_I]
1	0.981	8.5899e-05	[-73.136 -29.094 741.49]
2	0.98	0.0073391	[-132.36 -43.005 370.84]
3	0.99	0.0004143	[-183.92 -73.149 1012.4]
4	0.989	0.00032054	[-108.65 -36.08 660.37]
5	0.988	0.00035095	[-143.1 -79.248 938.06]
6	0.978	5.6416e-05	[-76.476 -63.128 960.58]

TABLE 2. Random control signal degradation.

Scenario Number		Random Selection		
		DG Number	Time (s)	Control Signal Degradation (%)
1	Case 1	DG1	at t = 7 s	40 %
	Case 2	DG5	at t = 8 s	30 %
2		DG2 and DG4 simultaneously	at t = 6 s and at t = 11 s simultaneously	20 % (DG2) 40 % (DG4)

capability have all been met. During random degradation of the control signal (actuator fault), the designed controllers are evaluated. Two scenarios are run through the study system with the proposed designed controls. The two scenarios are carried out using a random pick of such an actuator with fault level (control signal degradation in percentage) in a certain DG. The random selections are given in Table 2.

Scenario 1 (Random Actuator Fault in one DG):

Case 1: Actuator fault at DG1

The actuator in DG1 was chosen with 40% deterioration at t=7 s as shown in Table 2 by establishing a random selection technique and selecting a fault in one actuator with a random degradation level in a random time. Figure 3

$$\textit{minimize } tr(P_i)$$

$$\text{Subject to } \begin{bmatrix} -\alpha P_i & * & * & * & * & * \\ \hat{A}_{ii}P_i + \hat{B}_i Y_i & -P_i + \epsilon \hat{B}_i \hat{B}_i' + \rho F_A F_A' & * & * & * & * \\ 0 & \hat{D}_i' & -(1-\alpha) I_i + \gamma F_D F_D' & * & * & * \\ Y_i & 0 & \gamma F_D F_D' & -\epsilon I & * & * \\ H_A P_i & 0 & 0 & 0 & -\rho I & * \\ 0 & H_D & 0 & 0 & 0 & -\gamma I \end{bmatrix} \leq 0,$$

$$0 < \alpha < 1, \epsilon > 0, \rho > 0, \gamma > 0$$

$$\begin{bmatrix} -\alpha P_i & * & * & * \\ \hat{A}_{ii}P_i + \hat{B}_i Y_i & -P_i + \epsilon \hat{B}_i \hat{B}_i' & * & * \\ 0 & \hat{D}_i' & -(1-\alpha) I_i & * \\ Y_i & 0 & 0 & -\epsilon I \end{bmatrix} + \left(\begin{bmatrix} 0 \\ F_A \\ 0 \\ 0 \end{bmatrix} \Delta_A \begin{bmatrix} H_A & 0 & 0 & 0 \end{bmatrix} P_i + * \right)$$

$$+ \left(\begin{bmatrix} 0 \\ 0 \\ F_D \\ 0 \end{bmatrix} \Delta_D \begin{bmatrix} 0 & H_D & 0 & 0 \end{bmatrix} + * \right) \leq 0$$

$$\therefore \begin{bmatrix} -\alpha P_i & * & * & * \\ \hat{A}_{ii}P_i + \hat{B}_i Y_i & -P_i + \epsilon \hat{B}_i \hat{B}_i' & * & * \\ 0 & \hat{D}_i' & -(1-\alpha) I_i & * \\ Y_i & 0 & 0 & -\epsilon I \end{bmatrix}$$

$$+ \left(\rho \begin{bmatrix} 0 \\ F_A \\ 0 \\ 0 \end{bmatrix} \begin{bmatrix} 0 & F_A' & 0 & 0 \end{bmatrix} + \rho^{-1} \begin{bmatrix} P_i H_A' \\ 0 \\ 0 \\ 0 \end{bmatrix} \begin{bmatrix} H_A P_i & 0 & 0 & 0 \end{bmatrix} \right)$$

$$+ \left(\gamma \begin{bmatrix} 0 \\ 0 \\ F_D \\ 0 \end{bmatrix} \begin{bmatrix} 0 & 0 & F'_D & 0 \end{bmatrix} + \gamma^{-1} \begin{bmatrix} 0 \\ H_D' \\ 0 \\ 0 \end{bmatrix} \begin{bmatrix} 0 & H_D & 0 & 0 \end{bmatrix} \right) \leq 0$$

shows a fault in DG1 with a degradation in the control signal from 100% to 60%. The control signals for DG1, DG2, and DG3 before and after the fault occurrence are shown in Figure 3(a). During the fault instant, the fault consequences in DG2 and DG3 are minimal (% overshoot is ± 1.74 %). Moreover, Figure 3(c) provides the fault impacts in DG4, DG5, and DG6. The effects are close to zero. Fig. 3(c, d) shows the controlled output voltages of six DGs. Since the proposed tracker treats the fault as a disturbance, it completely solves the problem for DG1 (40% fault) with exceptional performance (it has 0.8% overshoot, 0.5 s settling time, and zero steady-state error). Furthermore, other trackers in the study system are shown in Figures 3(c, d) with significantly greater performance. Table 3 summarizes the implications of 40 % actuator fault in DG1 on the other five DGs. The control parameters shown in Table 3 demonstrate the dead-beat, quick, and zero steady-state performance of the designed trackers for the six DGs during the 40% fault in DG1.

Case 2: Actuator fault at DG5

The actuator in DG5 was selected with 30% degradation at t=8 s as presented in Table 1 by creating a random selection technique and picking a fault in one actuator with a random degradation level at a random time. Figure 4 displays a fault in DG5 with a fault in the control signal from 100% to 70%. Figure 4(a) depicts the control signals for DG1, DG2, and DG3 before and after the fault occurrence. The fault effects in DG1, DG2 and DG3 are negligible during the fault's occurrence. Furthermore, the largest influence of the fault (30% in DG5) occurs in the nearby DGs (DG4 and DG6)

$$A = \begin{bmatrix} 0.9951 & 0.03797 & 0.004429 & 6.703\,e-05 & 5.77\,e-06 & 7.51\,e-08 \\ -0.01315 & 0.9046 & -2.971\,e-05 & -3.045\,e-07 & -2.601\,e-08 & -2.563\,e-10 \\ 0.004429 & 8.58\,e-05 & 0.998 & 0.0297 & 0.002599 & 5.032\,e-05 \\ -1.49\,e-05 & -1.954\,e-07 & -0.006601 & 0.9045 & -8.736\,e-06 & -1.146\,e-07 \\ 5.77\,e-06 & 7.511\,e-08 & 0.002599 & 3.931\,e-05 & 0.998 & 0.03802 \\ -1.738\,e-08 & -1.713\,e-10 & -1.165\,e-05 & -1.194\,e-07 & -0.008802 & 0.9044 \\ 5.131\,e-09 & 5.033\,e-11 & 3.466\,e-06 & 3.523\,e-08 & 0.002662 & 5.153\,e-05 \\ -1.743\,e-11 & -1.376\,e-13 & -1.562\,e-08 & -1.202\,e-10 & -1.785\,e-05 & -2.341\,e-07 \\ 3.563\,e-12 & 2.805\,e-14 & 3.208\,e-09 & 2.458\,e-11 & 3.696\,e-06 & 4.809\,e-08 \\ -4.869\,e-15 & -3.209\,e-17 & -5.463\,e-12 & -3.37\,e-14 & -8.35\,e-09 & -8.228\,e-11 \\ 2.998\,e-15 & 1.971\,e-17 & 3.374\,e-12 & 2.075\,e-14 & 5.181\,e-09 & 5.082\,e-11 \\ -4.563\,e-18 & -2.581\,e-20 & -6.148\,e-15 & -3.165\,e-17 & -1.176\,e-11 & -9.29\,e-14 \end{bmatrix}$$

$$\begin{bmatrix} 5.131\,e-09 & 4.194\,e-11 & 3.563\,e-12 & 3.896\,e-14 & 2.998\,e-15 & 4.107\,e-17 \\ -1.743\,e-11 & -1.147\,e-13 & -9.712\,e-15 & -8.889\,e-17 & -6.826\,e-18 & -8.042\,e-20 \\ 3.466\,e-06 & 3.758\,e-08 & 3.208\,e-09 & 4.37\,e-11 & 3.374\,e-12 & 5.533\,e-14 \\ -7.83\,e-09 & -6.429\,e-11 & -5.463\,e-12 & -5.991\,e-14 & -4.611\,e-15 & -6.33\,e-17 \\ 0.002662 & 4.295\,e-05 & 3.696\,e-06 & 6.68\,e-08 & 5.181\,e-09 & 1.059\,e-10 \\ -1.193\,e-05 & -1.304\,e-07 & -1.113\,e-08 & -1.524\,e-10 & -1.176\,e-11 & -1.935\,e-13 \\ 0.9983 & 0.0317 & 0.002772 & 7.454\,e-05 & 5.827\,e-06 & 1.58\,e-07 \\ -0.0131 & 0.9046 & -1.858\,e-05 & -3.386\,e-07 & -2.626\,e-08 & -5.393\,e-10 \\ 0.002772 & 4.472\,e-05 & 0.9971 & 0.05279 & 0.004192 & 0.0001692 \\ -9.318\,e-06 & -1.019\,e-07 & -0.006599 & 0.9047 & -1.41\,e-05 & -3.854\,e-07 \\ 5.827\,e-06 & 6.321\,e-08 & 0.004192 & 0.0001128 & 0.9947 & 0.07908 \\ -1.756\,e-08 & -1.442\,e-10 & -1.88\,e-05 & -3.426\,e-07 & -0.008787 & 0.9042 \end{bmatrix}$$

$$B = \begin{bmatrix} 0.0002676 & 0.0 & 0.0 & 0.0 & 0.0 & 0.0 \\ 0.01318 & 0.0 & 0.0 & 0.0 & 0.0 & 0.0 \\ 0.0 & 0.0001049 & 0.0 & 0.0 & 0.0 & 0.0 \\ 0.0 & 0.006607 & 0.0 & 0.0 & 0.0 & 0.0 \\ 0.0 & 0.0 & 0.000179 & 0.0 & 0.0 & 0.0 \\ 0.0 & 0.0 & 0.00881 & 0.0 & 0.0 & 0.0 \\ 0.0 & 0.0 & 0.0 & 0.0002232 & 0.0 & 0.0 \\ 0.0 & 0.0 & 0.0 & 0.01318 & 0.0 & 0.0 \\ 0.0 & 0.0 & 0.0 & 0.0 & 0.0001865 & 0.0 \\ 0.0 & 0.0 & 0.0 & 0.0 & 0.006608 & 0.0 \\ 0.0 & 0.0 & 0.0 & 0.0 & 0.0 & 0.0003726 \\ 0.0 & 0.0 & 0.0 & 0.0 & 0.0 & 0.008809 \end{bmatrix}$$

C = unit matrix

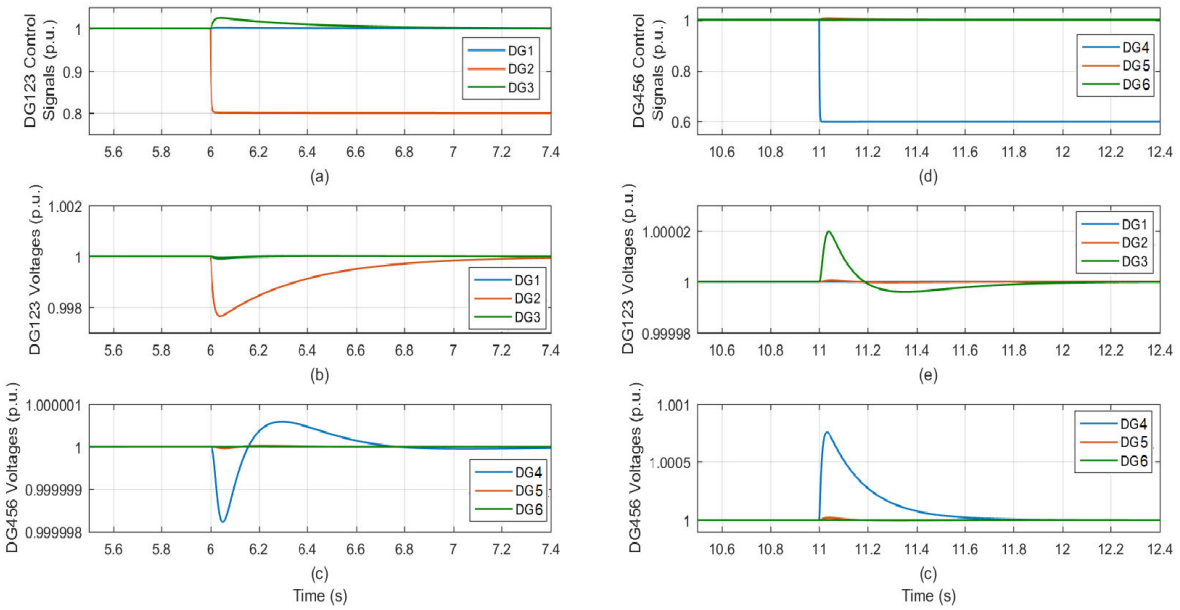

FIGURE 5. Degradation in the control signal of DG2 from 100% to 80% at $t = 6$ s and degradation on the control signal of DG4 from 100% to 60% at $t = 11$ s. (a) control signals for DG1, DG2 and DG3. (b, c).

TABLE 3. Control response parameters for the control signal and the trackers output voltages during fault 40 % in DG1.

		Control Response Parameters		
		% Overshoot (%)	Settling Time (s)	Steady State error (%)
Control Signal	DG1	NA	NA	NA
	DG2	1.74	0.221	≈ 0.0
	DG3	-0.6	0.1081	≈ 0.0
	DG4	0.005	0.1021	≈ 0.0
	DG5	0.001	0.0783	≈ 0.0
	DG6	0.00063	0.0734	≈ 0.0
Trackers Output Voltage	DG1	0.7881	0.497	≈ 0.0
	DG2	0.075	0.178	≈ 0.0
	DG3	0.00043	0.162	≈ 0.0
	DG4	0.000029	0.153	≈ 0.0
	DG5	0.0000064	0.137	≈ 0.0
	DG6	0.0000032	0.109	≈ 0.0

TABLE 4. Control response parameters for the control signal and the trackers output voltages during 30 % fault in DG5.

		Control Response Parameters		
		% Overshoot (%)	Settling Time (s)	Steady State error (%)
Control Signal	DG1	0	NA	0.000005≈ 0.0
	DG2	0.000002	0.672	0.000003≈ 0.0
	DG3	0.00789	0.681	≈ 0.0
	DG4	0.1223	0.692	≈ 0.0
	DG5	NA	NA	NA
	DG6	0.0124	0.676	≈ 0.0
Trackers Output Voltage	DG1	0.00000021	0.0856	≈ 0.0
	DG2	0.00000035	0.117	≈ 0.0
	DG3	0.00000786	0.1781	≈ 0.0
	DG4	0.000265	0.276	≈ 0.0
	DG5	0.275	0.596	≈ 0.0
	DG6	0.000277	0.269	≈ 0.0

reflecting on their effect to have less than 0.123% overshoot, as shown in Figure 4(c). The regulated output voltages of six DGs are shown in Figures 4 (c, d). Because of the suggested tracker handles the fault problem as a disturbance, it solves the problem with superior performance for DG5 (30% fault) (it has 0.275% overshoot, 0.596 s settling time, and zero steady-state error). In addition, other trackers in the study model with noticeably better performance are displayed in Figures 4 (c, d). The effects of 30% actuator fault in DG5 on the other five DGs are provided in Table 4. Table 4 shows the dead-beat, fast, and zero steady-state performance of the designed trackers for the six DGs during the 30% fault in DG.

Scenario 2 (Random Simultaneous Actuator Fault in Two DGs):

By developing a random selection technique and choosing a fault in two actuators simultaneous with a random deterioration level in a random time, the actuator in DG2 was selected with 20% degradation at t = 6 s and the actuator in DG4 was chosen with 40% at t = 11 s, as shown in Table 2. Figures 5 (a, b, c) show the first fault in DG2 with a control signal fault degradation from 100% to 80%, and Figures 5(d, e, f) show the second simultaneous fault in DG4 with a control signal fault from 100% to 60%. The control signals for DG1, DG2, and DG3 are shown in Figure 5(a) before and after the first fault occurrence. During the first fault occurrence in DG2, the fault effects appearing in neighboring DG1 and DG3 are minimal as given in Figure 6. Figures 5 (b, c) depict the controlled output voltages of six DGs. Since the proposed tracker treats the fault problem as a disturbance, it completely solves the problem while providing higher performance for DG2 (20% fault) (it has 0.232%

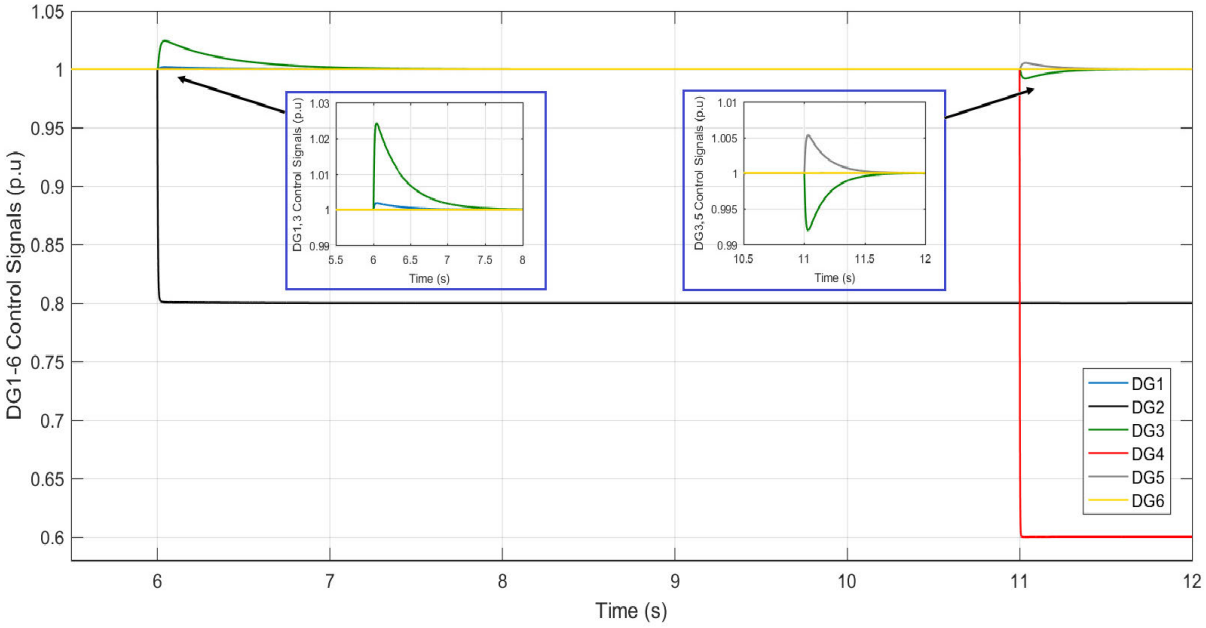

FIGURE 6. Control signals for six DGs during fault in two actuators simultaneously (DG2 with 20%, and DG4 with 40%.)

TABLE 5. Controlled output voltages response parameters in six DGs during fault in two actuators simultaneously (DG2 with 20%, and DG4 with 40%).

		Control Response Parameters					
		First Fault in DG2 (20%)			Second Fault in DG4 (40%)		
		% Overshoot (%)	Settling Time (s)	Steady State Error (%)	% Overshoot (%)	Settling Time (s)	Steady State Error (%)
Trackers Output Voltage	DG1	0.00182	0.631	≈ 0.0	0.000002531	0.8847	≈ 0.0
	DG2	0.232	0.8032	≈ 0.0	0.00006315	0.8321	≈ 0.0
	DG3	0.001134	0.6445	≈ 0.0	0.01973	0.7562	≈ 0.0
	DG4	0.0000725	0.6726	≈ 0.0	0.837	0.5641	≈ 0.0
	DG5	0.00000278	0.7036	≈ 0.0	0.00214	0.7383	≈ 0.0
	DG6	0.000000368	0.7218	≈ 0.0	0.0000769	0.8173	≈ 0.0

overshoot, 0.8032 s settling time, and no steady state error). Six DGs control response parameters during the first fault in DG2 is given in Table 5. The control signals for DG4, DG5, and DG6 are shown in Figure 5(d) before and after the second simultaneous fault occurrence. As shown in Fig. 6, during the second simultaneous fault in DG4, the fault impacts in neighboring DG3 and DG5 are negligible. The controlled output voltages of six DGs are shown in Figures 5(e, f). The recommended tracker totally solves the fault problem while giving higher performance for DG4 (40% fault). It has 0.837 % overshoot, 0.5641 s settling time, and no steady state error. Six DGs control response parameters during the second simultaneous fault in DG4 is given in Table 5. Table 5 depicts the extraordinary dead beat, swift, and zero steady state performance of the designed trackers for the six DGs when fault occurs in two actuators (DG2 with 20% and DG4 with 40%) simultaneously.

V. CONCLUSION

This paper introduced a novel approach for incorporating actuators faults into the design of passive FTC. The actuator faults are treated as uncertainties modelled in the norm-bounded form in the control input matrix. To address decentralization constraints, we decompose the global MG into multiple sub-grids, where each sub-grid controller minimizes the effects of the remaining system as an external

disturbance. The new derived theorem for tackling these conditions is obtained for PFTC. Those conditions are derived in terms of LMIs. In addition, a theorem is also derived to extend the previous results of microgrids which are subject to changing loads, modelled with norm-bounded parameter uncertainties. The proposed PFTC control is successful to stabilize the system even in the case of simultaneous occurrence of faults which is a very rare case to happen in practice. Moreover, the simulation results are obtained by randomly selecting an actuator/actuators with a fault- tolerant level (or, equivalently control signal degradation) in a specific DG. According to the IEEE standard, the proposed PFTC ensures robust stability, mandatory response, and steady-state capability. This work represents a significant step towards more robust and fault-tolerant control strategies for modern energy systems, with promising applications in various real-world scenarios.

APPENDIX: PROOF OF THEOREM 1 [21]

Consider the discrete-time dynamical system given by

$$x_{k+1} = Ax_k + Dw_k, z_k = Cx_k \tag{A1}$$

where the vectors x_k, w_k, z_k are the state, external disturbance, output to optimize of dimensions *n, m, l* respectively. The external disturbance w_k is l_∞-bounded satisfying the constraint

$$\|w_k\| \leq 1, \quad k = 0, 1, 2, \ldots \tag{A2}$$

System (A1) is assumed stable, (*A, D*) is controllable, and *C* is full-rank.

The ellipsoid

$$E_x = x_k' P^{-1} x_k \leq 1, \quad P > 0 \tag{A3}$$

centered at the origin is termed state-invariant if for an initial condition $x_0 inside E_x$ implies x_k will not leave the ellipsoid for the future time *k=0,1,2,..* Also, for trajectories starting outside E_x will be attracted to this ellipsoid as time evolves (ellipsoid is also attracting). We have the following.

Theorem [21]: The ellipsoid E_x is state-invariant, and attracting, for (A1) if and only if the following LMI is satisfied

$$\left.\begin{array}{l} \frac{1}{\alpha} APA' - P + \frac{1}{1-\alpha} DD' \leq 0, \ subject\ to \\ P > 0, \qquad\qquad\qquad\qquad scalar\ 0 > \alpha > 1 \end{array}\right\} \tag{A4}$$

Proof: Consider the Lyapunov function

$$V_k = x_k' Q x_k, Q > 0, \quad Q = P^{-1} \tag{A5}$$

The trajectories x_k will not leave the ellipsoid, $E_x = V_k \leq 1$ if and only if

$$V_{k+1} \leq 1, subject\ to\ V_k \leq 1, w_k' w_k \leq 1 \tag{A6}$$

Condition (A6) along with (A1) can be re-written as

$$\left.\begin{array}{l} (Ax_k + Dw_k)' A (Ax_k + Dw_k) \leq 1\ subjet\ to \\ x_k' Q x_k \leq 1, \quad w_k' w_k \leq 1 \end{array}\right\} \tag{A7}$$

(A7) can be combined into a single matrix inequality, using the S-procedure, as

$$\begin{bmatrix} A'QA - \alpha Q & * \\ D'QA & D'AD - \beta I \end{bmatrix} \leq 0, \quad \alpha + \beta \leq 1 \tag{A8}$$

Without loss of generality, $\beta = 1 - \alpha$.

Using the state feedback $u = Kx$, and replacing A with $A+BK$ in (A8) results in theorem 1. (Q.E.D)

REFERENCES

[1] F. A. El-Sheikhi, H. M. Soliman, R. Ahshan, and E. Hossain, "Regional pole placers of power systems under random failures/repair Markov jumps," *Energies*, vol. 14, no. 7, p. 1989, Apr. 2021.

[2] H. M. Soliman, F. A. El-Sheikhi, E. H. E. Bayoumi, and M. De Santis, "Ellipsoidal design of robust stabilization for Markov jump power systems under normal and contingency conditions," *Energies*, vol. 15, no. 19, p. 7249, Oct. 2022, doi: 10.3390/en15197249.

[3] M. Blanke, M. Kinnaert, J. Lunze, and M. Staroswiecki, *Diagnosis and Fault-Tolerant Control*, 3rd ed. Heidelberg, Germany: Springer, 2016.

[4] M. S. Mahmoud and Y. Xia, *Analysis and Synthesis of Fault-Tolerant Control Systems*. Hoboken, NJ, USA: Wiley, 2014.

[5] N. Derbel, J. Ghommam, and Q. Zhu, *Diagnosis, Fault Detection & Tolerant Control*. Singapore: Springer, 2020.

[6] H. Noura, D. Theilliol, J.-C. Ponsart, and A. Chamseddine, *Fault-tolerant Control Systems: Design and Practical Applications*. London, U.K.: Springer-Verlag, 2009.

[7] S. Ding, *Advanced Methods for Fault Diagnosis and Fault-Tolerant Control*. Berlin, Germany: Springer-Verlag, 2021.

[8] H. Alwi, C. Edwards, and C. P. Tan, *Fault Detection and Fault-Tolerant Control Using Sliding Modes*. London, U.K.: Springer-Verlag, 2011.

[9] H. Shen, L. Su, and J. H. Park, "Reliable mixed H_∞/passive control for T-S fuzzy delayed systems based on a semi-Markov jump model approach," *Fuzzy Sets Syst.*, vol. 314, pp. 79–98, May 2017.

[10] H. R. Patel and V. Shah, "Fuzzy logic based passive fault tolerant control strategy for a single-tank system with system fault and process disturbances," in *Proc. 5th Int. Conf. Electr. Electron. Eng. (ICEEE)*, May 2018, doi: 10.1109/ICEEE2.2018.8391342.

[11] M. Benosman and K.-Y. Lum, "Passive actuators' fault-tolerant control for affine nonlinear systems," *IEEE Trans. Control Syst. Technol.*, vol. 18, no. 1, pp. 152–163, Jan. 2010.

[12] T. A. Johansen and T. I. Fossen, "Control allocation—A survey," *Automatica*, vol. 49, pp. 1087–1103, May 2013.

[13] X. Yu and J. Jiang, "A survey of fault-tolerant controllers based on safety-related issues," *Annu. Rev. Control*, vol. 39, pp. 46–57, Jan. 2015.

[14] L. I. Allerhand and U. Shaked, "Robust switching-based fault tolerant control," *IEEE Trans. Autom. Control*, vol. 60, no. 8, pp. 2272–2276, Aug. 2015.

[15] A. Abbaspour, K. K. Yen, P. Forouzannezhad, and A. Sargolzaei, "An adaptive resilient control approach for pressure control in proton exchange membrane fuel cells," *IEEE Trans. Ind. Appl.*, vol. 55, no. 6, pp. 6344–6354, Nov. 2019.

[16] M. Salimifard and H. A. Talebi, "Robust output feedback fault-tolerant control of non-linear multi-agent systems based on wavelet neural networks," *IET Control Theory Appl.*, vol. 11, no. 17, pp. 3004–3015, Nov. 2017.

[17] E. Bayoumi, M. Soliman, and H. M. Soliman, "Disturbance-rejection voltage control of an isolated microgrid by invariant sets," *IET Renew. Power Gener.*, vol. 14, no. 13, pp. 2331–2339, Oct. 2020, doi: 10.1049/iet-rpg.2019.1019.

[18] K. M. Bhargavi, N. S. Jayalakshmi, D. N. Gaonkar, A. Shrivastava, and V. K. Jadoun, "A comprehensive review on control techniques for power management of isolated DC microgrid system operation," *IEEE Access*, vol. 9, pp. 32196–32228, 2021.

[19] M. S. Mahmoud, *MICROGRID: Advanced Control Methods and Renewable Energy System Integration*. Amsterdam, The Netherlands: Elsevier, 2017.

[20] J. Kumar, A. Agarwal, and V. Agarwal, "A review on overall control of DC microgrids," *J. Energy Storage*, vol. 21, pp. 113–138, Feb. 2019.

[21] M. V. Khlebnikov, B. T. Polyak, and V. M. Kuntsevich, "Optimization of linear systems subject to bounded exogenous disturbances: The invariant ellipsoid technique," *Autom. Remote Control*, vol. 72, no. 11, pp. 2227–2275, Nov. 2011.
[22] H. M. Soliman, E. H. E. Bayoumi, F. A. El-Sheikhi, and A. M. Ibrahim, "Ellipsoidal-set design of the decentralized plug and play control for direct current microgrids," *IEEE Access*, vol. 9, pp. 96898–96911, 2021, doi: 10.1109/ACCESS.2021.3094896.
[23] *IEEE Recommended Practice for Monitoring Electric Power Quality*, Standard IEEE Standard 1159-2009, Revision IEEE Standard 1159-1995, Jun. 2009, pp. 1–94, doi: 10.1109/IEEESTD.2009.5154067.

HISHAM M. SOLIMAN received the B.Sc. (Hons.) and M.Sc. degrees in electrical engineering from Cairo University, Cairo, Egypt, in 1972 and 1975, respectively, and the Ph.D. degree in automatic control from Paul Sabatier University, Toulouse, France, in 1980. He is currently a Professor of electrical engineering with Cairo University. He taught at the University of Saskatchewan, Canada; Garyounis University, Libya; United Arab Emirates University (UAEU), United Arab Emirates; the Yanbu Industrial College, Saudi Arabia; and Sultan Qaboos University, Oman.

EHAB H. E. BAYOUMI received the B.Sc. degree in electrical power engineering from Helwan University, Egypt, in 1988, the M.Sc. degree in electrical power engineering from Ain Shams University, Egypt, in 1996, and the Ph.D. degree in electrical power engineering from Cairo University, Cairo, Egypt, in, 2001. He has been with the Electronic Research Institute (ERI), Cairo, since 1990. From 2000 to 2001, he joined LUT, Finland, as a Visiting Researcher. He was appointed as an Assistant Professor with the Chalmers University of Technology, Sweden, from 2003 to 2005. In 2008, he was appointed as an Associate Professor with ERI, where he was appointed as a Full Professor, in 2014. He is currently a Full Professor with The British University in Egypt. He was with the Yanbu Industrial College, Saudi Arabia; the Higher Colleges of Technology, United Arab Emirates; the University of Eswatini, Eswatini; and Egyptian Chinese University, Egypt. His research interests include high-performance ac machines, power quality, switching power converters in smart and microgrids, and nonlinear control applications in power electronics, smart grids, and electric drive systems. He was the Editor-in-Chief of the *International Journal of Industrial Electronics and Drives*, in 2013.

FARAG ALI EL-SHEIKHI received the M.Sc. degree in power system simulation from the University of Missouri, Columbia, USA, and the Ph.D. degree in power systems reliability evaluation from the University of Saskatchewan, Canada. He was a Professor of electrical energy and power system reliability with the University of Benghazi, Libya. He is currently a Teaching Staff with the Electrical and Electronics Engineering Department, Faculty of Engineering and Architecture, Istanbul Esenyurt University, Istanbul, Turkey. His research interests include power generation systems, transmission and distribution networks planning, operation, and maintenance, and he has many publications in these areas. He has a special interest in the development and implementation of the reliability-centered maintenance (RCM) approach, PAS-55, and ISO 55000/1/2 asset management international standards. He has successfully implemented such techniques and standards in electrical power utilities. The implementation of such techniques and standards for power utilities, petroleum, petrochemical, and heavy industries will result in useful life extension of all equipment and a huge saving in the organization's investment and cost-effectiveness. Successful implementation of RCM and ISO 55001 Standard will lead to the enhancement of the organization's physical assets reliability and efficiency; making a significant impact on profits and shareholders value through productivity, quality, and system reliability. Moreover, it will lead to asset uptime improvement, better system availability, less forced, and unnecessary planned outages, and a greater understanding of the level of system risk that the organization is managing; leading to an upgrading of operating procedures and systems strategies.

RAZZAQUL AHSHAN (Senior Member, IEEE) received the B.Sc. degree in electrical and computer engineering from the Khulna University of Engineering and Technology, Bangladesh, in 2002, and the M.Eng. and Ph.D. degrees in electrical engineering from the Memorial University of Newfoundland, St. John's, NL, Canada, in 2008 and 2013, respectively, with a scholarship from the Natural Sciences and Engineering Research Council of Canada (NSERC). He was a Lecturer for three years with the Khulna University of Engineering and Technology. In 2011, he joined the College of North Atlantic, Newfoundland, Canada, as a Faculty Member and a Researcher, until August 2016. He is currently an Associate Professor with the Department of Electrical and Computer Engineering, Sultan Qaboos University (SQU), Muscat, Oman. His research interests include machines, power electronic converters, renewable energy systems, microgrids, smart grids, engineering optimization, energy management and control, energy storage, virtual synchronous generator, green hydrogen, and digital signal processing techniques and their applications in power systems. He was a recipient of the 2021 Distinguished Academician Award from SQU, a fellow of the School of Graduate Studies, Memorial University of Newfoundland, in 2013, and the Prime Minister Gold Medal Award from KUET, Bangladesh, in 2002. He is an Associate Editor of IEEE TRANSACTIONS ON INDUSTRY APPLICATIONS. He is also ranked Top 2% of World's Researchers, in 2023 (Stanford University and Elsevier).

SARVAR HUSSAIN NENGROO received the master's degree in electrical engineering from Pusan National University, Republic of Korea. He is currently pursuing the Ph.D. degree with the Cho Chun Shin Graduate School of Mobility, Korea Advanced Institute of Science and Technology, Republic of Korea. He was a Guest Researcher with the Technical University of Denmark. His research interests include renewable energy aggregation, microgrids, electric vehicles, and power electronics.

SANGKEUM LEE received the B.S. degree in electronics and information engineering from Korea University, in 2016, and the M.S. and Ph.D. degrees from the CCS Graduate School for Green Transportation, Korea Advanced Institute of Science and Technology (KAIST), in 2018 and 2020, respectively. He was a Postdoctoral Researcher with the Mechanical Engineering Research Institute, KAIST, in 2021. He was a Senior Researcher of the Electronics and Telecommunications Research Institute, ETRI, in 2023. He is currently an Assistant Professor with the Department of Computer Engineering, Hanbat National University. His main research interests include sensor network systems and their supporting technologies, such as optimization, deep learning, sensor networks, and industrial energy systems.